Journal of Structural Geology, Vol. 5, No. 6, pp. 591 to 601, 1983
Printed in Great Britain

0191-8141/83 $03.00 + 0.00
Pergamon Press Ltd.

New aspects of rhomb structures

DOV BAHAT

Department of Geology and Mineralogy,
The Ben-Gurion University of the Negev, Beer Sheva, Israel

(*Received* 9 *December* 1982; *accepted in revised form* 4 *July* 1983)

Abstract—The acute angles of 48 rhombic, trapezoidal and triangular grabens, horsts and upthrusts throughout the world were determined. The results indicate an angular spread of 7–73°. In most structures the two acute angles differ considerably. Most rhomb structures are grabens which show affinities to seismic faults, and only a few are horsts and upthrusts. In this connection modes of static crustal fracture propagation are compared to dynamic propagation. Rhomb structures occur along strike-slip faults and in rifts. These results question the universality of the pull-apart model as a mechanism for rhomb structure development. The two mechanisms that can lead to the formation of rhomb structures are (1) interaction of en échelon or non-coplanar fractures by shear and extensional modes and (2) fracture bifurcation in an extensional mode. The two mechanisms may result in faults of different shapes characterized by curved and straight boundaries, respectively. The grabens and horsts in extensional regions are the consequence of early fracture and later vertical displacements.

INTRODUCTION

FOLLOWING earlier models by Quennell (1958) and Carey (1958) many rhomb grabens (or pull-apart basins) and rhomb upthrusts (horsts) have been described along strike-slip (wrench) faults throughout the world. Investigators have considered a variety of mechanisms to explain pull-apart structures. Wilcox *et al.* (1973) observed these structures in relation to convergent and divergent wrenching. Opposed crustal blocks that do not move parallel with a wrench fault either converge or diverge as wrenching proceeds. When convergence occurs, compression along reverse and strike–slip faults results in high-angle thrusting. On the other hand, divergent wrenching results in an overlay of extensional block faulting with consequent grabens along high-angle normal faults. Crowell (1974) and Livaccari (1979) presented a model of up- and down-tilted wedges and pull-apart basins along a dextral wrench fault zone. The deformation in the Basin and Range province of the U.S.A. was explained by this mechanism. Apparently, N-trending pull-apart grabens formed in a wide dextral shear zone at 45° to the NW-trending wrench faults. Tchalenko & Berberian (1975) showed the development of a graben in an extensional gap which occurred due to left-lateral shear between two left-stepping en échelon faults. This idea was further elaborated by Segall & Pollard (1980). Dewey (1982) considered pull-apart basins as derivatives of the inherent complexities related to the evolution of strike-slip systems, in a plate tectonics context. Such structures may show all transitions from a graben floor of slightly stretched continental crust, through severely attenuated continental crust, to an oceanic floor. Aydin & Nur (1982) analysed 70 well defined rhomb-like pull-apart basins and pressure ridges along major strike-slip fault systems. They observed that these basins become wider as they grow longer with increasing fault offset.

Although many rhomb structures previously described are considered to be 'well-defined' (Aydin & Nur 1982), this is not at all clear. Quite often, fault boundaries of rhomb structures are inferred rather than (carefully) mapped, and the strike-slip mechanism suggested for their origin is not certain. For instance, although the Ocotillo Badlands have been mentioned as a typical rhomb upthrust, one notes the qualified description of the faults which surround this structure (Sharp & Clark 1972 p. 137). Freund, a strong advocate of the rhomb-shaped graben concept along the Dead Sea Rift (Freund *et al.* 1968) expresses his concerns about the validity of the model (Freund 1978). He observed that the Ayun graben is not rhombic but triangular, and its dimensions are far too small (compared with the strike-slip requirement), whereas the Lake Kineret (Sea of Galilee) graben is several times too long and is extra wide in the north. Freund (1978) speculated that these difficulties may be partly resolved by rotating the eastern side of the rift 3° anticlockwise around a pivot situated between the Hula and Kineret grabens, and by bending Galilee (the region on the west side of the rift between Hula and Kineret). However, these adjustments would result in overlaps between the rhomb structures that cannot be easily explained. Furthermore, Freund recognized that these adjustments do not resolve the significance of a flexure northeast of Lake Kineret. Finally, it should be mentioned that the faults originally proposed around Lake Kineret (Freund *et al.* 1968) do not quite fit data obtained during more recent geological (Bartov 1979) and geophysical (Folkman 1980) studies. For example, recent detailed mapping of the Bir Zreir graben in Eastern Sinai (Bartov *et al.* 1983) has raised doubts regarding the role of strike-slip displacements in connection with the development of the rhomb. These are only a few examples (see Aydin & Nur 1982, table 1), that demonstrate deviations from a clear agreement regarding the conventional concept of rhomb structure development along strike-slip faults.

Characterization of a rhomboid requires the determination of its angles. In the present study 89 acute angles of 48 rhomboidal, trapezoidal and trianglar structures throughout the world are determined. These are analysed, the affinities of these structures with seismic faults and rifts are evaluated, and the mechanical significance of them is discussed.

ASSUMPTIONS

A recent study has shown that extensional aspects of earthquake-induced ruptures in Southern California can be characterized by an analysis of crack bifurcation and interaction according to fracture mechanics principles (Bahat 1982). Similar assumptions to those made in that study can be made for the present analysis of rhomb-structures. Basically, these assumptions claim that fracture propagation and interaction leading to the evolution of rhomb-structures can be modelled by elastic theories and simulated by small-scale experiments (in glass and granite). The applicability of such assumptions to structural problems has been repeatedly demonstrated (e.g. Delaney & Pollard 1981).

DETERMINATION OF ACUTE ANGLES OF RHOMB STRUCTURES

The accuracy of angular determinations in a rhomb-structure is a function of the scale and accuracy of the map on which the measurement is made. In detailed maps accuracy can be ±2° or better (Bahat 1982). Most maps used in the present study, however, lack some details of the faults and accuracy is reduced to ±5°, but this is not thought to be critical. More important are relative values of the two acute angles of a given rhomb-structure. Therefore, in spite of the above limitation, the angular results given in Table 1 are significant.

Table 1. Characterization of 48 rhomb structures

Rhomb location	Graben (G) Horst (H) Upthrust (U)	Actual shape of structure	Acute angle (deg.)	Acute angle (deg.)	Width (m)	Predominant fracture regime	Reference (structure)	Reference (seismic)
(1)	(2)	(3)	(4)	(5)	(6)	(7)	(8)	(9)
Rio El Tambor, Montagua f., Guatamala	G	Trapezoid	19	36	20	shear	Schwartz *et al.* (1979)	Langer & Bollinger (1979)
Lake Izabel, Polochic f., Guatamala	G	Rhomboid	26	28	20,000	shear	Plafker (1976)	Langer & Bollinger (1979)
La Gonzaler, Bocono f., Venezuela	G	Rhomboid	18	26	4,000	shear?	Schubert (1980)	Dewey (1972)
Casanay, El Pilar f., Venezuela	G	Rhomboid	34	42	900	shear	Schubert (1979)	Dewey (1972)
Olinghouse f., Sierra Nevada, U.S.A.	G	Rhomboid	61	68		shear	Sanders & Slemmons (1979)	
	G	Triangle	18			shear	Sanders & Slemmons (1979)	
Olinghouse f., Sierra Nevada, U.S.A.	G (large)	Rhomboid	49	30	200	shear	Aydin & Nur (1982)	
	G (small)	Rhomboid	48	53	40	shear		
Southern Basin and Range, U.S.A.	G	Rhomboid	38	49		shear?	Crowell (1974), Stewart (1978)	Scholz *et al.* (1971)
	U	Triangle	23			shear?	Crowell (1974), Stewart (1978)	
Espanola basin, Rio Grande rift, U.S.A.	G	Trapezoid	32	54	15,000	shear	Golombek (1981)	
Imperial–Brawley faults, S. California, U.S.A.	G	Trapezoid	39	62	7,000	shear	Johnson & Hadley (1976)	Johnson & Hadley (1976)
Imperial–Brawley faults, S. California, U.S.A.	G	Rhomboid	47	41	7,000	shear	Hill (1977)	Sharp (1976)
Imperial f., Salton Sea, California, U.S.A.	G	Rhomboid	38	10	7,000	shear	Fuis *et al.* (1981)	Sharp (1976)
Coyote Creek f., San Jacinto f., S. California, U.S.A.	U	Rhomboid	54	59	2,000	shear	Sharp & Clark (1972)	Allen & Nordquist (1972)
Coyote Creek f., San Jacinto f., S. California, U.S.A.	G	Rhomboid	33	73	200	shear	Bahat (1982)	Allen & Nordquist (1972)
	G	Triangle	33		400	shear	Bahat (1982)	Allen & Nordquist (1972)
Upper Angara rift, Baikal rift, U.S.S.R.	G	Rhomboid	42	45	30,000	extension	Logatchev (1978); Logatchev & Florensov (1978)	Logatchev *et al.* (1978)
Tsipa-Bount rift, Baikal rift, U.S.S.R.	G	Rhomboid	20	24	20,000	extension	Logatchev (1978); Logatchev & Florensov (1978)	Logatchev *et al.* (1978)
New Lake Baikal rift, Baikal rift, U.S.S.R.	G	Triangle	20		17,000	extension	Logatchev (1978); Logatchev & Florensov (1978)	Logatchev *et al.* (1978)

Table 1. (continued)

Rhomb location	Graben (G) Horst (H) Upthrust (U)	Actual shape of structure	Acute angle (deg.)	Acute angle (deg.)	Width (m)	Predominant fracture regime	Reference (structure)	Reference (seismic)
(1)	(2)	(3)	(4)	(5)	(6)	(7)	(8)	(9)
Dasht-e-Bayaz, Iran	G	Rhomboid	26	32	500	shear	Ambraseys & Tchalenko (1969)	Ambraseys & Tchalenko (1969)
Erzican, North Anatolia, Turkey	G	Triangle (distorted)	8	21	3,500	shear	Aydin & Nur (1982)	
Syria	G	Rhomboid	42	45	1,800	shear	Garfunkel *et al.* (1982)	
Marj Ayun, Yammuneh f., Lebanon	G	Triangle	32	66	1,600	shear	Freund *et al.* (1968)	Ben-Menahem *et al.* (1976)
Hula basin, Israel	G	Trapezoid	57	69	7,000	shear	Freund *et al.* (1968)	Ben-Menahem *et al.* (1976)
Dead Sea, Israel	G	Rhomboid	37	60	12,000	shear	Quennell (1958)	Wu *et al.* (1973)
Timna, Israel	G	Rhomboid	34	35	250	shear	Freund *et al.* (1968)	
Bir Zreir, Sinai	G	Rhomboid	33	51	1,500	shear	Eyal *et al.* (1981)	
Tiran–Dakar, Gulf of Elat	G	Rhomboid	44	48	8,000	shear	Ben-Avraham *et al.* (1979)	
Aragonese, Gulf of Elat	G	Rhomboid	31	44	9,000	shear	Ben-Avraham *et al.* (1979)	
Elat, Gulf of Elat	G	Rhomboid	46	56	10,000	shear	Ben-Avraham *et al.* (1979)	
West of Belayim oil, Gulf of Suez	G	Rhomboid	41	72	7,000	extension	Garfunkel & Bartov (1977)	
SE-Escarpment Ethiopia	G	Triangle	41		1,200	shear	Juch (1980); Mohr (1967)	Laughton (1965)
	G	Rhomboid	26	37	2,000	shear	Juch (1980); Mohr (1967)	
	G	Rhomboid	25	54	2,000	shear	Juch (1980); Mohr (1967)	
Lake Turkana, N. Kenya (10? my)	G	Rhomboid	13	26	70,000	extension	Cerling & Powers (1972)	
Central Gregory rift, Kenya	H	Rhomboid	43	48	420	extension	King (1978); Griffiths (1980)	Tobin *et al.* (1969)
	H	Rhomboid	43	43	500	extension	King (1978); Griffiths (1980)	Molnar & Aggarwal (1971)
	H	Rhomboid	35	43	450	extension	King (1978); Griffiths (1980)	Molnar & Aggarwal (1971)
	H	Rhomboid	36	61	1,300	extension	King (1978); Griffiths (1980)	Molnar & Aggarwal (1971)
	G	Rhomboid	27	37	800	extension	King (1978); Griffiths (1980)	Molnar & Aggarwal (1971)
	H	Rhomboid	55	58	600	extension	King (1978); Griffiths (1980)	Molnar & Aggarwal (1971)
Lebtema Block, N. Tanzania	H	Rhomboid		53	26,000	extension	King (1978)	Wohlenberg (1970)
Mbozi block, S. Tanzania	H	Triangle	18		36,000	extension	King (1978)	Wohlenberg (1970)
Hanmer Springs, Hope f., New Zealand	G	Rhomboid	31	37	6,000	shear	Freund (1974)	Scholz (1977)
Awatore f., New Zealand	G	Rhomboid	34	43	2,000	shear	Freund (1974)	Scholz (1977)
Vestfold–Ringerike graben, Norway	G	Rhomboid	59	63	70,000	shear?	Ramberg & Larsen (1978)	Husebye & Ramberg (1978)
Akersbus graben, Oslo graben, Norway	G	Rhomboid	55	56	50,000	shear?	Ramberg & Larsen (1978)	Husebye & Ramberg (1978)

THEORETICAL BACKGROUND

Interaction of bifurcating cracks

When crack bifurcation occurs, a single fracture is divided into two branches that propagate separately, under combined loading of tension (mode I) and longitudinal shear (mode II). Kalthoff (1972) has shown that in *Araldite B* (polymeric glass) these branches interact with one another, and each crack deviates by an angle γ from its original direction following bifurcation (Fig. 1). This angle can be determined from Erdogen & Sih (1963) by

$$K_{II}/K_{I} = \sin\gamma/3\cos\gamma - 1, \qquad (1)$$

where K_I and K_{II} are the stress intensity factors for modes I and II, respectively. Kalthoff has also shown that for forks with small branch angles $\alpha < \alpha_c$ where α_c is approximately 14°, the propagation of the branches tends to enlarge the angle. For forks with larger branch angles, $\alpha > \alpha_c$, the propagation of the branches tends to diminish the angle. Forks with the critical angle α_c will propagate in their original direction. Bahat (1982) elaborated on this crack interaction and showed that branching of rapid ruptures induced by the earthquakes in the crust in southern California followed the angular relationships observed by Kalthoff (1972). This branching process led to the development of two grabens.

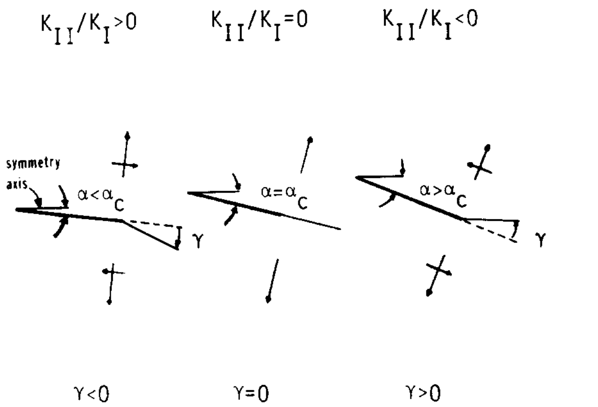

Fig. 1. Three possible propagation paths of a branch crack in a symmetric fork. Only one branch and the symmetry axis are shown. Straight arrows indicate near field stresses. The branch angle, α, is shown between two curved arrows, and γ is the deviation angle from the initial propagation path (after Kalthoff 1972, fig. 4).

Interaction between non-coplanar opposing cracks under tensile loading

A different crack interaction is one which occurs about opposing or overlapping parallel cracks (Fig. 2a). Yokobori *et al.* (1971) investigated the interaction between two non-coplanar opposing parallel elastic cracks under tensile loading. Their theoretical analysis was in good agreement with experimental results derived from experiments on cellophane paper. They investigated the case when K_A and K_B are tensile stress intensity factors at points A and B, respectively (Fig. 2a), and K is the stress intensity factor of an isolated tensile crack. Generally, K_A is smaller than both K_B and K when overlap is present due to relatively high stress relaxation. K_B is greater than K except when overlap is large. They also found that the stress intensity factors of shear stress produced by the interaction are considerably smaller than those of tensile stress. During the interaction between the cracks, when small overlap is present, the crack tips at A and A' deviate away from each other. When large overlap is present these tips approach each other. Swain & Hagan (1978) observed similar interactions between such cracks in soda-lime glass (Fig. 2b). They established that the angular deviation from straight-line growth for these cracks may also be determined by equation (1).

Whereas fracture interaction associated with bifurcating cracks (Fig. 1) appears to be along straight lines which bend at sharp angles, interactions between non-coplanar opposing cracks characteristically occur along curves. Swain & Hagan (1978, fig. 2c) have demonstrated experimentally that these two interaction styles may occur under extensile loading at close proximities.

Interaction between non-coplanar opposing cracks under shear loading

Krantz (1979) examined fracture interaction under shear loading in granite. He investigated non-coplanar crack arrays (which he called '*en passant*') and found a resemblance to the results obtained under tensile loading by Swain & Hagan (1978). The crack paths were determined by the local K_{II}/K_I ratios (K_{II} and K_I being the stress intensity factors of the longitudinal shear and tension mode, respectively), such that deviations from planar propagation increased as the ratio increased.

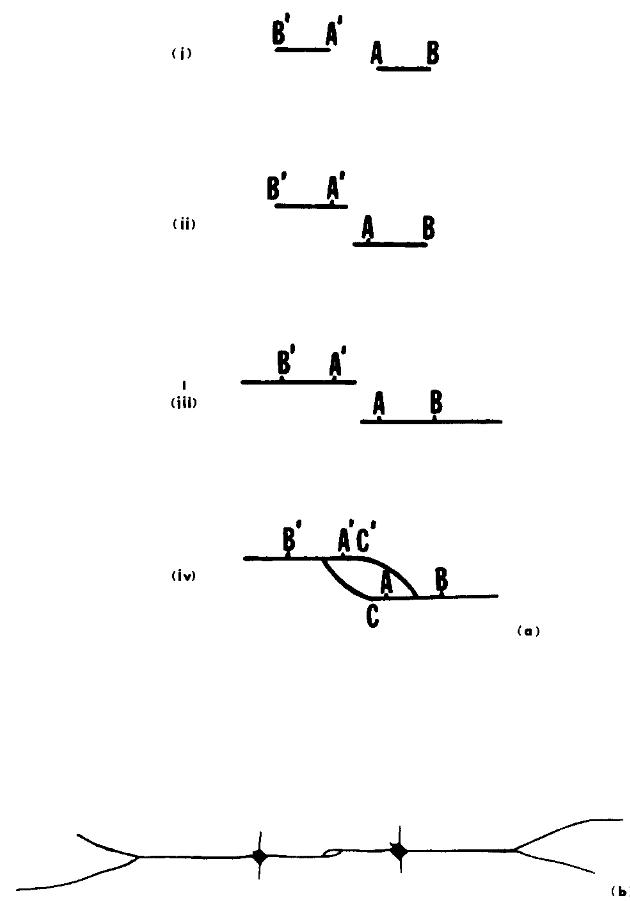

Fig. 2. Experimental crack interaction. (a) Schematic illustration of propagation behaviour of two non-coplanar parallel cracks. Inner tips of both cracks are A and A', and outer tips are B and B'. Stage (i) decribes cracks before overlapping. At stage (ii) propagation from A and A' is shown. At stage (iii) overlap is attained, propagation stopping at A and A' and proceeding from B and B'. Stage (iv) represents a finite body. After the arrival of B and B' at the edges of specimen, interaction from C and C' proceeds (after Yokobori *et al.* 1971, fig. 26). (b) Two parallel cracks caused by indentation (at two large black spots) are stimulated by a stress wave. This stimulation induces fracture propagation (at 300 m $^{-1}$). At the centre there is an interaction between two non-coplanar cracks. Prior to overlap the cracks deviate slightly away from each other, then they grow towards each other and join. Propagation away from each other leads to bifurcation. Distance separating the cracks 10 μm. Distance between indentations 210 μm (after Swain & Hagany 1978, fig. 1c).

Two styles of en échelon cracks

The criteria for the definition and classification of en échelon cracks in the crust are not yet settled. If it is postulated that these cracks are the products of mixed mode fracturing (tension and shear), a basic characteristic feature would be segmentation of a large straight fracture to small parallel straight cracks oriented at an acute angle to the former (Allen *et al.* 1972, Sharp 1976, Delaney & Pollard 1981, fig. 20, Bahat 1982). This segmentation mostly occurs close to the crustal surface

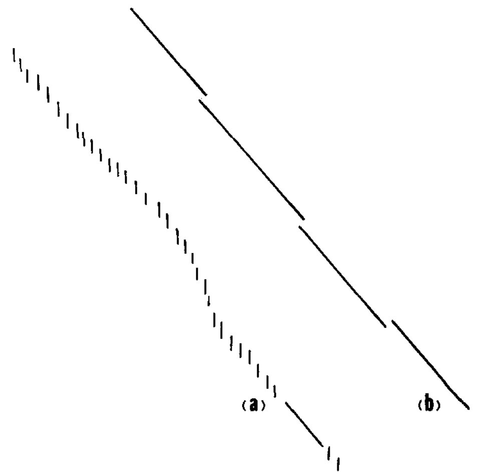

Fig. 3. Two styles of en échelon cracks. (a) Segmentation of a large fracture into small parallel cracks oriented obliquely to the large fracture. (b) A series of parallel fractures, some of them arranged en échelon.

(Sharp 1976). The above en échelon cracks (Fig. 3) differ significantly from straight large en échelon fractures which are nearly parallel with the general trend of the fault (Segall & Pollard 1980). The latter may not represent mixed-mode fractures and it is not at all clear that they reflect the actual mechanical segmentation. Schulman (1959) characterized 'longitudinal rows' of N–S en échelon (step) faults which are parallel to the Dead Sea Rift. Such fractures require a different explanation. Extensional aspects of fractures along the Dead Sea Rift are discussed in a separate study (Bahat & Rabinovitz 1983). However, mechanical interaction between tips of en échelon cracks of these two groups show some resemblances.

Interactions between en échelon cracks under shear loading

Krantz (1979) found that under shear loading, interaction of en échelon cracks is controlled by both mode I and mode II. Segall & Pollard (1980) found that in a pair of en échelon right-stepping cracks under right-lateral shear, extension fractures would form near the crack tips and propagate into the region between the cracks, possibly linking them. They also suggested the existence of a wide zone of potential shear failure between the cracks, which partly overlaps with the zone of extensional failure. In the extension field the direction of propagation depended on the magnitude of the ratio K_{II}/K_I (see also Delaney & Pollard 1981).

It was observed that under remote tension, crustal fractures may follow equation (1) (Bahat 1982). It is yet to be established what are the minimum extensional conditions to maintain the dependence of the directions of interacting cracks on equation (1) under shear loading.

Shapes of interacting cracks under extension and shear loading

Interacting bifurcating cracks under extension seem to be straight (Bahat 1982). Non-coplanar cracks under tensional loading seem to interact along curved trajectories (Fig. 2a). Experimental en échelon and non-coplanar cracks under shear loading seem to show interactions along curved and straight paths. Judging by numerical calculations of stress distribution close to crack tips (Kranz 1979, fig. 3, Segall & Pollard 1980, fig. 9) paths of interaction should be curved. However, experimental results (Bombolakis 1968, Krantz 1979) show straight fracture propagation. Apparently, under conditions of strong remote uniaxial compression oblique to the initial crack, further propagation becomes straight and occurs parallel to the compression direction, and the actual crack interaction by local stresses is suppressed. Therefore, it is possible that in a set-up in which remote compression is not dominant, crack interaction should assume the expected curve paths.

RESULTS

The results in Table 1 are indicative of the following features.

(1) There is a wide spreading of acute angles (Fig. 4) in the 7–73° range (Table 1, columns 4 and 5). There is no trend towards a maximum, although there seems to be a poorly defined concentration increase from the peripheries of this range towards the centre.

(2) There is no correlation between widths (column 6), the sizes of structures (Aydin & Nur 1982) and values of acute angles of rhomboids.

(3) In most structures the two acute angles differ considerably and only in a few rhomboids are the two angles approximately equal.

(4) Rhomboidal shapes are the most common, but, there are also trapezoids and triangles (column 3).

(5) Most structures are grabens and only a few are horsts (upthrusts) (column 2).

(6) Most rhomboidal structures have affinities to seismic faults (note references in column 9).

(7) Rhomboidal structures occur along strike-slip systems and also in rifts (column 7). The shear regime is disputed in a few structures by question marks (note references in column 8).

The significance of these observations is elaborated in the following sections.

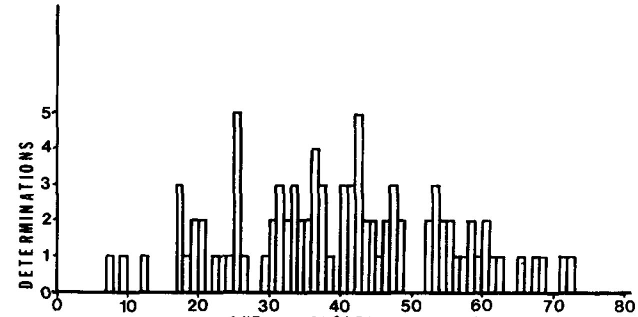

Fig. 4. Frequency histogram for acute angles of rhomb structures, showing the wide angular spread for various structures.

SPREAD OF ACUTE-ANGLE VALUES OF RHOMBOIDS

Quennell (1958), in his early model of the formation of the Dead Sea, described the mechanism of block displacement from two pre-existing subparallel major faults and a bridging oblique fault. He did not explain the process or processes that produced these faults. Recently, in reference to faults in California, Segall & Pollard (1980) elaborated on the mechanisms that have led to the development of bridging oblique faults (secondary fracturing). They considered that the major faults were two pre-existing segments from an en échelon array (nearly parallel with the general trend of the regional faults). Following the analyses of interactions between such fracture pairs by Yokobori *et al.* (1971), Swain & Hagan (1978) and Kranz (1979) in the laboratory (see theoretical background) and Segall & Pollard (1980) in the crust, it becomes clear that the bridging path of the oblique fault (Fig. 5) is determined by the combined effects of the local tensile and shear stresses. As these combined effects will vary from location to location, so will the shape of the oblique bridging fault. This may explain the wide angular range of acute angles of pull-apart grabens (Table 1, Fig. 4) if the above mechanism based on interaction between fracture pairs is adopted. Each acute angle represents an intersection between a segment of the en échelon or non-coplanar array and an oblique bridging fault. The acute angle appears to be independent of the width and size of the graben or horst (Table 1).

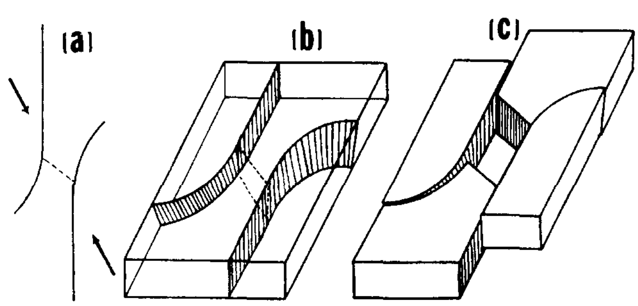

Fig. 5. Block diagram showing in idealized form the mechanism for the formation of the Dead Sea rhomb graben. (a) The fault pattern in plan. Arrows show the direction of compressive stress, solid lines are the two sub-parallel major faults and the dashed line is the bridging oblique fault. (b) The block before movement. (c) The block after movement (after Quennell 1958, fig. 1).

INEQUALITY OF ACUTE ANGLES IN RHOMBOIDS

Following the conventional model of strike-slip displacement that results in a pull-apart basin (Fig. 5), the single oblique fault that bridges the two en échelon fractures becomes the plane from which the two blocks detach along opposite directions parallel to the regional orientation of the strike-slip fault. This requires equality of the two acute angles of the pull-apart basin, with only minor deviations due to possible block rotation (6° in the case of the Dead Sea according to Quennell 1958). The large deviations from equality in many structures (Table 1) question the validity of the pull-apart model as a universal mechanism. With this model it is also difficult to explain the presence of triangular and trapezoidal grabens (and horsts).

A mechanism that can produce rhomboidal grabens (see theoretical background) and horsts (as well as triangles and trapezoidal structures) by extension rather than shear can be derived from a previous analysis by Bahat (1982). According to this mechanism, extension fractures may bifurcate (especially under dynamic conditions). If there is a single fork comprising extensional bifurcating fractures a triangular graben or horst may be developed. If however, two bifurcating fracture forks propagate towards each other, their approach or intersection may result in either rhomboidal or trapezoidal structures (Fig. 6). Such a mechanism is independent in both forks and does not require the equality of the two acute angles in a rhomboid. As such, it fits the results shown in Table 1 better than the pull-apart model.

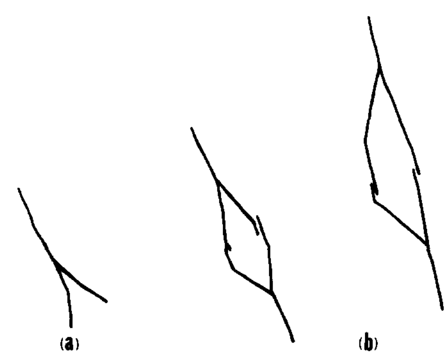

Fig. 6. Extensional fractures bifurcate and produce conditions for various rhomb structures to develop. (a) A single bifurcation develops into a triangle structure. (b) Two bifurcations which approach each other may result into a rhomboidal (left) or a trapezoidal (right) structure (also see Bahat 1982, fig. 5).

Most rhomboids are grabens and only few are horsts: dynamic conditions

Table 1 shows that most structures are grabens and only a few are horsts (also see Aydin & Nur 1982, table 1). This is unexpected in terms of conventional hypotheses of pull-apart basin evolution, because there is no reason why examples of right-lateral shear and right-stepping (Segall & Pollard 1980) should be common and instances of right-lateral shear and left-stepping should be rare.

This unexpected feature can possibly be correlated with an interesting observation made by Segall & Pollard (1980). They found that earthquake swarms and aftershocks cluster near right steps along right-lateral faults, related to grabens (such an observation was not made in relation to upthrusts). They also correlated the seismic activities with secondary fracturing in the Imperial Valley. Assuming that these observations can be generalized this may lead to two suggestions. (1) Grabens are more common than upthrusts because they are products of extensional conditions. Such conditions

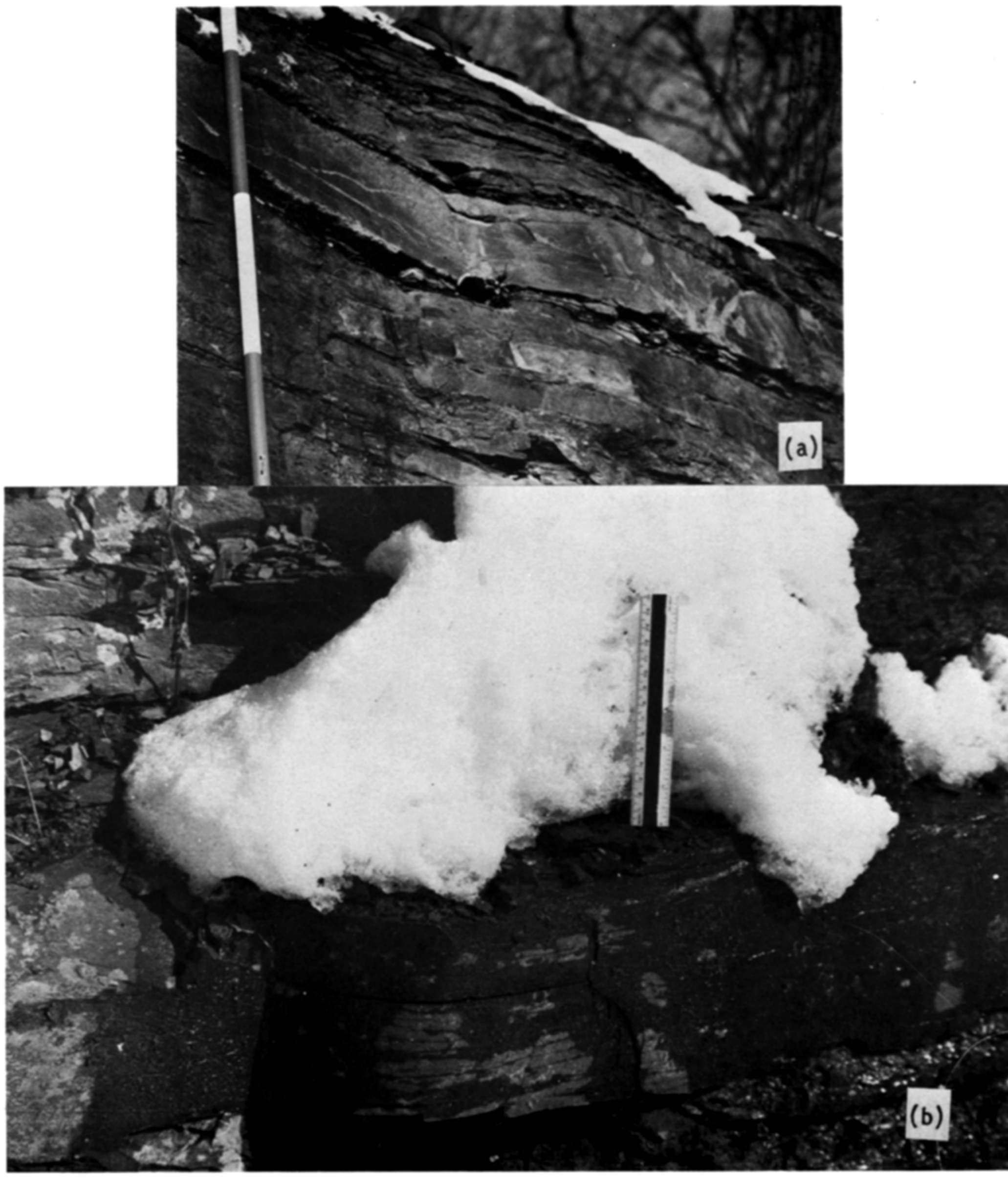

Fig. 7. Joint interaction in siltstone beds, in the Appalachian Plateau. (a) Sub-asymptotical curve abutting. (b) Sub-perpendicular curve abutting.

encourage seismic activity that produces secondary fracturing. The same seismic activity is not encouraged apparently in right-lateral left-stepping environments which are compressive, therefore, no fault bifurcations occur and upthrusts are rare. (2) It appears that the evolution of pull-apart basins is closely associated with seismic activity. Many of the examples given in Table 1 (column 9) are clearly connected with faults with strong affinities to earthquakes. This implies that in connection with rhomboid evolution the relevant models for fracture propagation and interaction should mostly be dynamic (although some slow seismic activities are known as well). This is manifested by the wide range of acute angle values in grabens and horsts (upthrusts) (Table 1). Dynamic conditions are expected to allow a wide range of mode I (tension)/mode II (shear) ratios (Bahat 1982) which would determine the propagation direction of the bridging oblique faults, and ultimately the acute angle of the pull-apart graben.

Fracture under static conditions

In order to appreciate crustal fracture interaction under dynamic conditions, one wants to compare it with fracture interaction under static conditions. The latter may show significant differences. Two examples of crustal fracture interaction are shown in Fig. 7. These are two representatives from a series of joint interactions in Upper Devonian siltstones in the Appalachian Plateau of New York. Here, fracture interaction occurs under conditions of slow fracture propagation (presumed stress corrosion, Bahat & Engelder, in preparation). Figure 7 shows two interactions between parallel joints. One joint propagated (horizontally) and when it overlapped the existing other straight-joint it curved towards it. Curving is at a small angle, almost asymptotically oriented as illustrated in Fig. 7(a). In Fig. 7(b) curving terminates at a large angle, almost perpendicularly. Under conditions of very slow propagation one parallel fracture can be thought of as a free boundary at which the shear stress is zero (and the principal stresses parallel and perpendicular to the boundary). Therefore, the abutting fracture (the second fracture) is likely to meet the existing surface either asymptotically or perpendicularly. Rapid fracture propagation on the other hand, would have been diverted from small or large angles due to the various influences of shear and due to inertia. This would result in a wide range of acute angles between 0 and 90° as shown in Table 1.

Rhomboid structures in rifts

One of the most intriguing observations is the common presence of rhomboidal, trapezoidal and triangular grabens and horsts in rifts along which strike-slip is either small or insignificant (Table 1) (e.g. the Baikal rift, the Gulf of Suez and several structures along the East African rift system, in particular, the Gregory rift). In the Baikal rift, horizontal displacements along fault planes were essentially negligible, not more than 1.0–1.5 km (Sherman 1978) along a rift of more than 1000 km in length. The extensile aspects of the East African rifts (including the Gulf of Suez) are well known (McConnell 1967) and do not need further elaboration.

It is significant that the pull-apart grabens along the Bocono fault zone in the Venezuaelan Andes (Table 1) are considered by Schubert (1980) to reflect shear processes. This however is disputed by the observations by Renz (1956), Shagam (1972), Murphy & Graubard (1977) and Giegengack (1977). According to these authors these grabens were formed in a zone of normal faulting. There is no consensus regarding the shear mechanisms in the Basin and Range grabens and horsts (Stewart 1978). Also, there are both shear and extensional characteristics in the Oslo graben (Ramberg & Larsen 1978). It is not known if these are exceptional or typical observations for rhomboidal structures associated with strike-slip faults.

Table 1 does not reveal any angular differences between the rhomboidal structures associated with great shear displacements (e.g. the southern Californian and Dead Sea systems) and those located in extensile regions. This suggests that either the rhombic structures in both stress regions are ultimately products of similar mechanisms, or alternatively, the products of shear and extensional mechanisms may give rise to comparable angular relationships. An analogous question was raised by Şengör & Burke (1978) regarding rifting being the product of either extension or shear. It is also possible that the absence of obvious angular differences result from the lack of precise details about the faults presumed to bound some rhomboidal structures. Future studies may supply the answers to these problems. An obvious question here is, if pull-apart structures have not resulted from remote shear in the rifts, how could they be produced by remote extension? Such a development can be the consequence of a two stage process by which an early extensile fracture is followed by vertical movements. Only such a process can explain the ubiquity of rhomboidal horsts (which supposedly reflect compression stresses) in the Gregory rift. Presumably, mantle diapirism in Kenya (Baker & Wohlenberg 1971) has been responsible for pushing up the already fractured blocks. As mentioned above, some scientists that have theorized about the development of the rhomboidal structures (e.g. Quennell 1958, Freund 1965, Segall & Pollard, 1980) assumed existing sub-parallel fractures before displacement.

A rhombic structure in a strike-slip regime

The rhomb graben that occurs where the Brawley fault system meets the Imperial fault system in southern California (Fig. 8) has attracted considerable attention. The faults around the graben are the products of both extension and shear (Sharp 1976, Hill 1977). Furthermore, a detailed map by Johnson & Hadley (1976) shows two straight bifurcating branches of the Brawley fault system (the Brawley fault and fault A manifested by epicentres). These faults are being approached from

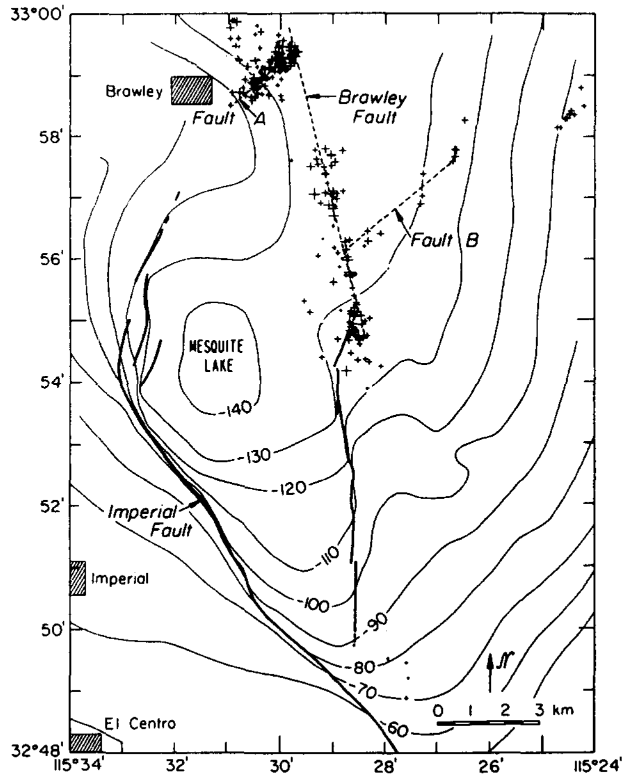

Fig. 8. Detailed map (after Johnson & Hadley 1976) showing the graben surrounded by the Brawley and Imperial fault systems. Plus signs are epicentres (January, 1975 earthquake), heavy lines represent observed surface faulting, dashed lines are seismically inferred faults, and thin lines are topographic contours.

the south by two branches of the Imperial fault system. The eastern branches of the two faults are fairly straight. The western branch of the Imperial fault, on the other hand, starts as a straight fracture and continues along a curved trajectory as it interacts with the Brawley fault system. Hence, the fault boundaries of this graben exhibit both straight bifurcating fractures controlled mostly by extension (Bahat 1982), and curved faults which responded to shear stresses on non-coplanar fractures (faults).

Thus, two fracture mechanisms that can lead to the development of pull-apart basins have been discussed. The conventional strike-slip model is based on fracture interaction between crack-pairs. Such a mechanism is likely to result in grabens (and other related structures) possibly with curved boundaries if there is not uniaxial-dominant (horizontal) compression. The other mechanism is based on fracture bifurcation under extensional conditions. According to the latter model graben boundaries are expected to be straight with sharp angular perimeters (Fig. 6). Both mechanisms are expected to occur naturally and thus I conclude that in future more attention should be paid to the detailed mapping of fault boundaries of rhomboid structures. This may enable us to distinguish between the two mechanisms. Swain & Hagan (1978) have experimentally shown the close association of the two patterns (Fig. 2b). Figure 8 demonstrated these two mechanisms in close proximity to each other in the crust.

Acknowledgements—I would like to thank Zvi Ben-Avraham who read the first draft and made important comments that helped to improve the manuscript.

REFERENCES

Allen, C. R. & Nordquist, J. M. 1972. Foreshock, main shock, and larger after-shocks of the Borrego Mountain earthquake. *Prof. Pap. U.S. geol. Surv.* **787**, 16–23.

Allen, C. R., Castle, R. O., Clarke, M. M., Grantz, A., Sharp, R. V., Theodore, T. G., Wolfe, E. W., Young, T. L. 1972. Map showing surface ruptures created at the time of and after the Borrego Mountain Earthquake of April 9, 1968 (G.M.T.) *Prof. Pap. U.S. geol. Surv.* **787**, plate 1.

Ambraseys, N. N. & Tchalenko, J. S. 1969. The Dasht-e Bay̌az (Iran) earthquake of August 31, 1968: a field report. *Bull. seism. Soc. Am.* **59**, 1751–1792.

Aydin, A. & Nur, A. 1982. Evolution of pull-apart basins and their scale independence. *Tectonics* **1**, 91–105.

Bahat, D. 1982. Extensional aspects of earthquake induced ruptures determined by an analysis of fracture bifurcation. *Tectonophysics* **83**, 163–183.

Bahat, D. & Rabinovitch, A. 1983. The initiation of the Dead Sea Rift. *J. Geol.* **91**, 307–322.

Baker, B. H. & Wohlemberg, J. 1971. Structure and evolution of the Kenya Rift Valley. *Nature, Lond.* **229**, 538–542.

Bartov, J. 1979. *Israel-Geologic map*, 1:500,000. Geological Survey of Israel.

Bartov, Y., Steinitz, G., Eyal, Y., Eyal, M. & Folkman. 1983. The development of rhomb-shaped grabens in Eastern Sinai. *Ann. Meet. Israel Geol. Soc.* **8**.

Ben-Avraham, Z., Almagor, G. & Garfunkel, Z. 1979. Sediments and structure of the Gulf of Elat (Aqaba)—Northern Red Sea. *Sediment. Geol.* **23**, 239–267.

Ben-Menaham, A., Nur, A. & Vered, M. 1976. Tectonics, seismicity and structure of the Afro-Eurasian junction—the breaking of an incoherent plate. *Phys. Earth Planet. Interiors* **12**, 1–50.

Bombolakis, E. G. 1968. Photoelastic study of initial stages of brittle fracture in compression. *Tectonophysics* **6**, 461–473.

Carey, S. W. 1958. The tectonic approach to continental drift. In: *Continental Drift* (edited by Casrey, S. W.). University of Tasmania Geology Department Symposium. No. 2, Hobart, 177–355.

Cerling, T. E. & Powers, D. W. 1977. Paleorifting between the Gregory and Ethiopian rifts. *Geology* **5**, 441–444.

Crowell, J. C. 1974. Origin of Late Cenozoic basins in southern California. In: *Tectonics and Sedimentation* (edited by Dickinson, W. R.). *Spec. Publs Soc. econ. Paleont. Miner., Tulsa* **22**, 190–204.

Delaney, P. T. & Pollard, D. D. 1981. Deformation of host rocks and flow of magma during growth of minette dikes and breccia-bearing intrusions near Ship Rock, New Mexico. *Prof. Pap. U.S. geol. Surv.* **1202**, 1–61.

Dewey, J. M. 1972. Seismicity and tectonics of western Venezuela. *Bull. seism. Soc. Am.* **62**, 1711–1751.

Dewey, J. F. 1982. Plate tectonics and the evolution of the British Isles. *J. geol. Soc. London* **139**, 371–412.

Erdogen, F. & Sih, G. C. 1963. On the crack extension in plates under plane loading and tranverse shear. *J. Basic Engng Trans. ASME* **D85**, 519–527.

Eyal, M., Eyal, Y., Bartov, Y. & Steinitz, G. 1981. The tectonic development of the western margin of the Gulf of Elat (Aqaba) Rift. *Tectonophysics* **80**, 39–66.

Folkman, Y. 1980. Magnetic and gravity investigations of the Dead Sea rift and adjacent areas in northern Israel. *J. Geophys.* **48**, 34–39.

Freund, R. 1965. A model of the structural development of Israel and adjacent areas since Upper Cretaceous times. *Geol. Mag.* **102**, 189–205.

Freund, R. 1974. Kinematics of transform and transcurrent faults. *Tectonophysics* **21**, 93–134.

Freund, R. 1978. The concept of a sinistral megashear. In: *Lake Kineret* (edited by Serruya, C.). *Monog. Biol. W. Junk Pub. The Hague* **32**, 27–31.

Freund, R., Zak, I. & Garfunkel, Z. 1968. Age and rate of the sinistral movement along the Dead Sea rift. *Nature, Lond.* **220**, 253–255.

Fuis, G. S., Mooney, W. D., Healy, J. H., McMechan, G. A. & Lutter, M. J. 1981. Seismic-refraction studies of the Imperial Valley region, California-profile models, a travel-time contour map, and a gravity model. Open-File Rep. 81-270.

Garfunkel, Z., Zak, I. & Freund, R. 1982. Active faulting in the Dead Sea Rift. *Tectonophysics* **80**, 1–26.

Garfunkel, Z. & Bartov. V. 1977. The tectonics of the Suez Rift. *Geol. Surv. Isr. Bull.* **71**, 1–44.

Giegengack, R. 1977. Late-Cenozoic tectonics of the Tabay–Estanques graben Venezuelan Andes. In: *Memorias del V Congreso Geologico Venezolano* (edited by Expejo, A.). Ministerio de Energia y Minas, Caracas, Vol. 2, 721–737.

Golombek, M. P. 1981. Geometry and rate of extension across the Pajarito fault zone, Española basin, Rio Grande rift, northern New Mexico. *Geology* **9**, 21–24.

Griffiths, P. S. 1980. Box-fault systems and ramps: atypical associations of structures from the eastern shoulder of the Kenya rift. *Geol. Mag.* **117**, 576–586.

Hill, D. P. 1977. A model for earthquake swarms. *J. geophys. Res.* **82**, 1347–1352.

Hill, D. P., Mowinckel, P. & Peake, L. G. 1975. Earthquakes, active faults, and geothermal areas in the Imperial Valley, California. *Science Wash.* **188**, 1306–1308.

Husebye, E. S. & Ramberg, I. B. 1978. Geophysical investigations. In: *The Oslo Paleorift* (edited by Dons, J. A. & Larsen, B. T.). *Norges geol. Unders.* **337**, 41–53.

Johnson, C. E. & Hadley, D. M. 1976. Tectonic implications of the Brawley earthquake swarm, Imperial Valley, California, January 1975. *Bull. seism. Soc. Am.* **66**, 1133–1144.

Juch, D. 1980. Tectonics of the southeastern escarpment of Ethiopia. In: *Geodynamic Evolution of the Afro-Arabic Rift System*. Academic Nazionale Dei lincei **47**, 407–418.

Kalthoff, J. F. 1972. On the propagation direction of bifurcated cracks. In: *Dynamic Crack Propagation* (edited by Sih, G. S.). Noordhoff, Leyden, 449–458.

King, B. C. 1978. A comparison between the older (Karroo) rifts and the younger (Cenozoic) rifts of eastern Africa. In: *Tectonics and Geophysics of Continental Rifts* (edited by Ramberg, I. B. & Neumann, E.-R.). Reidel Company, Dordrecht, Holland, 347–350.

Kranz, R. L. 1979. Crack–crack and crack–pore interactions in stressed granite. *Int. J. Rock Mech. Min. Sci. Geomech. Abstr.* **16**, 37–47.

Langer, C. J. & Bollinger, G. A. 1979. Secondary faulting near the terminus of seismogenic strike-slip fault: after shocks of the 1976 Guatemala earthquake. *Bull. seism. Soc. Am.* **69**, 427–444.

Laughton, A. S. 1965. The gulf of Aden, in relation to the Red Sea and the Afar depression of Ethiopia. In: *The World Rift System* (edited by Irvine, T. N.). *Geol. Surv. Pap. Can.* **66–14**, 78–97.

Livacarri, R. F. 1979. Late Cenozoic tectonic evolution of the western United States. *Geology* **7**, 72–75.

Logatchev, N. A. 1978. Main features of evolution and magmatism of continental rift zones in the Cenozoic. In: *Tectonics and Geophysics of Continental Rifts* (edited by Ramberg, I. B. & Neumann, E. R.). Reidel Company, Dordrecht, Holland, 351–366.

Logatchev, N. A. & Florensov, N. A. 1978. The Baikal system of rift valleys, *Tectonophysics* **45**, 1–13.

Logatchev, N. A., Rogozhina, V. A., Solonenko, V. P. & Zorin, Yu. A. 1978. Deep structure and evolution of the Baikal rift zone. In: *Tectonics and Geophysics of Continental Rifts* (edited by Ramberg I. B. & Neumann, E. R.). Reidel Company, Dordrecht, Holland, 49–61.

McConnell, R. B. 1967. The East African rift system. *Nature, Lond.* **215**, 578–581.

Mohr, P. A. 1967. Major volcano-tectonic lineament in the Ethiopian rift system. *Nature, Lond.* **18**, 664–665.

Molnar, P. & Aggarwal, Y. P. 1971. A micro-earthquake survey in Kenya. *Bull. seism. Soc. Am.* **61**, 195–201.

Murphy, D. & Graubard, C. 1977. Structural relations of the northeastern termination of the Tabay–Estanques graben, central Venezuelan Andes. In: *Memorias del V Congreso Geologica Venezolano* (edited by Espejo, A.). Ministerio de Energia y Minas, Caracas, Vol. 2, 715–720.

Plafker, G. 1976. Tectonics aspects of the Guatemala earthquake of 4th February 1976. *Science, Wash.* **193**, 1201–1208.

Quennell, A. M. 1958. The structural and geomorphic evolution of the Dead Sea Rift. *Q. Jl. geol. Soc. Lond.* **114**, 1–24.

Renz, O. 1956. Cretaceous in western Venezuela and the Guajira (Columbia). *Preprint, 20th Int. geol. Congr., Mexico* 1–13.

Ramberg, I. B. & Larsen, B. I. 1978. Tectonomagmatic evolution. In: *The Oslo Paleorift* (edited by Dons, J. A. & Larsen, B. T.). *Norges geol. Unders.* **337**, 55–73.

Sanders, C. & Slemmons, D. B. 1979. Recent crystal movement in the Central Sierra Nevada–Walker Lane region of California–Nevada—Part III. The Olinghouse fault zone. *Tectonophysics* **52**, 585–597.

Scholz, C. H. 1977. Transform fault systems of California and New Zealand: similarities in their tectonic and seismic styles. *J. geol. Soc. Lond.* **133**, 215–229.

Scholz, C. H., Barazangi, M. & Sbar, M. L. 1971. Late Cenozoic evolution of the Great Basin, Western United States, as an ensialic interarc basin. *Bull. geol. Soc. Am.* **82**, 2979–2990.

Schubert, C. 1979. El Pilar fault zone, northeastern Venezuela: brief review. *Tectonophysics* **52**, 447–455.

Schubert, C. 1980. Late-Cenozoic pull-apart basins, Boconó fault zone, Venezuelan Andes. *J. Struct. Geol.* **2**, 463–468.

Schulman, N. 1959. The geology of the Central Jordan Valley. *Bull. Res. Counc. of Israel* **8G**, 63–90.

Schwartz, D. P., Cluff, L. S. & Donnelly, T. W. 1979. Quaternary faulting along the Caribbean–North American plate boundary in Central America. *Tectonophysics* **52**, 431–445.

Segall, P. & Pollard, D. D. 1980. Mechanics of discontinuous faults. *J. geophys. Res.* **85**, 4337–4350.

Şengör, A. M. C. & Burke, K. 1978. Relative timing of rifting and volcanism on earth and its tectonic implications. *Geophys. Res. Lett.* **5**, 419–421.

Shagam, R. 1972. Evolution tectonica de los Andes Venezolanos. *Spec. Publs Bol. geol. Caracas* **2**, 1201–1261.

Sharp, R. V. 1976. Surface faulting in Imperial Valley during the earthquake swarm of January–February, 1975. *Bull. seism. Soc. Am.* **66**, 1145–1154.

Sharp, R. V. & Clark, M. M. 1972. Geologic evidence of previous faulting near the 1968 rupture on the Coyote Creek fault. *Prof. Pap. U.S. geol. Surv.* **787**, 131–140.

Sherman, S. I. 1978. Faults of the Baikal rift zone. *Tectonophysics* **45**, 31–39.

Stewart, J. H. 1971. Basin and Range structure: a system of horsts and grabens produced by deep-seated extension. *Bull. geol. Soc. Am.* **82**, 1019–1044.

Swain, M. V. & Hagan, J. T. 1978. Some observations of over-lapping interacting cracks. *Engng Fract. Mech.* **10**, 299–304.

Tchalenko, J. S. & Berberian, M. 1975. Dasht-e Bayaz fault, Iran: earthquake and earlier related structures in bed rock. *Bull. geol. Soc. Am.* **86**, 703–709.

Tobin, D. G., Ward, P. L. & Drake, C. L. 1969. Microearthquakes in the rift valley of Kenya. *Bull. geol. Soc. Am.* **80**, 2043–2046.

Wilcox, R. E., Harding, T. P. & Seely, D. R. 1973. Basin wrench tectonics. *Bull. Am. Ass. Petrol. Geol.* **57**, 74–96.

Wohlenberg, J. 1970. On the seismicity of the East African Rift System. In: *Graben Problems* (edited by Illies, J. H. & Mueller, St.). International upper Mantle Project Sci. Rep. 27, 290–295.

Wu, F. T., Karcz, I., Arieh, E. J., Kafri, U. & Peled, U. 1973. Micro-earthquakes along the Dead Sea Rift. *Geology* **1**, 159–161.

Yokobori, T., Uozomi, M. & Ichikawa, M. 1971. Interaction between non-coplanar parallel staggered elastic cracks, *Rep. Res. Inst. Strength Fract. Mater. Tohoku Univ.* **7**, 25–47.